ISSN (Print) 1226-1750
ISSN (Online) 2233-6656
Journal of Magnetics 24(1), 43-48 (2019) https://doi.org/10.4283/JMAG.2019.24.1.043

Effect of Gd Substitution on the Structural, Magnetic, and Magnetocaloric Properties of $Fe_{68}Tb_5B_{23}Nb_4$ Metallic Glass

Ersin Civan[1], Kagan Sarlar[2,3], and Ilker Kucuk[2]*

[1]*National Defence University, Air Non-Commissioned Officer (NCO) Higher Vocational School, 35415, Gaziemir-İzmir, Turkey*
[2]*Physics Department, Faculty of Arts and Sciences, Uludag University, Gorukle Campus 16059 Bursa, Turkey*
[3]*Physics Department, Kamil Ozdag Faculty of Sciences, Karamanoglu Mehmetbey University, Yunus Emre Campus, 70100 Karaman, Turkey*

(Received 29 May 2018, Received in final form 22 December 2018, Accepted 27 December 2018)

The effects of adding Gd on the Curie temperature (T_C), glass-forming ability (GFA), and magnetocaloric effect (MCE) were studied in $Fe_{68-x}Gd_xTb_5B_{23}Nb_4$ (x = 0, 2, and 6) glassy alloys prepared by suction casting. It was shown that when Gd content was exchanged with Fe partially for x = 2, GFA was increased, whereas for x = 6, adding Gd content has reduced the GFA and amorphous structure could not be obtained. Critical diameter was found to be 3 mm for $Fe_{66}Gd_2Tb_5B_{23}Nb_4$ bulk metallic glass (BMG). By exchanging Gd with Fe partially, T_C could effectively be tuned in a quite broad temperature interval from 487 K (x = 0) to 380 K (x = 6) for which amorphous structure could not be obtained. Maximum magnetic entropy change $(-\Delta S_M)^{max}$ values were found to be 1.16, 0.84 $Jkg^{-1}K^{-1}$, and 0.54 $Jkg^{-1}K^{-1}$ as well as, refrigeration capacity (RC) values were obtained as 116 J/kg, 84.84 J/kg, and 40.50 J/kg under a low field change of 2 T for x = 0, 2, and 6, respectively. Although T_C was shifted to lower temperatures by exchanging Fe with Gd partially, $-(\Delta S_M)^{max}$ decreased almost half of the base alloy and RC decreased approximately 1/3 of the base alloy.

Keywords : Metallic glasses, Gd, magnetocaloric effect, magnetic entropy change

1. Introduction

MCE is the heating up and cooling down phenomenon of magnetic materials with the varying magnetic field (i.e. magnetisation and demagnetisation) [1, 2]. Discovering giant MCE in $Gd_5Si_2Ge_2$ [3], $LaFe_{11.4}Si_{1.6}$ [4] and $MnFe_{0.95}P_{0.67}Si_{0.33}$ [5] alloys encourages researchers to search for better magnetic materials having MCE because of their potential use in magnetic refrigeration (MR) technologies. Nearly 17 % of the overall electricity used worldwide is consumed by the refrigeration sector including air conditioning [6]. Hence, efficiency in using energy is very important. Refrigeration based on MCE has relatively high energy efficiency as well as its reasonable cost (30 % possible energy saving with respect to conventional cooling technologies). In addition, since there is no need to use ozone-depleting gasses, the harmful environmental impacts can be reduced by using MR technologies [7]. Low working frequency (0.2-10 Hz) [8] of magnetic refrigerators is another reason to be interested in magnetocaloric materials. In addition to its use in refrigeration, MCE also can be used in the treatment of cancer cells through heating of cancer cells by applying a variable magnetic field [9].

Large MCE can be obtained near the vicinity of magnetic or magneto-structural phase transitions. Magnetocaloric materials are classified as materials having first order magneto-structural phase transition (FOMT) and second order magnetic transition (SOMT) according to the type of phase transitions. The fundamental differences between first-order and second-order phase transitions are that second-order phase transition is the continuous change of the magnetisation around the Curie temperature while in the first-order phase transition the magnetisation does not change continuously. In addition, in the second-order phase transitions, the magnetic entropy change increases in the larger magnetic fields, whereas in the first-order phase transitions, the magnetic entropy values increase only at the certain magnetic field values. While MCE can be observed in a wide temperature range, it is

*Corresponding author: Tel: +902242941703
Fax: +902242941899, e-mail: ikucuk@uludag.edu.tr

important to obtain MCE near working temperature. Although MCE has been carried out near or above room temperature which is important in daily life technology since 1950s, its commercial application has just begun.

Pure Gd, which exhibits large MCE near room temperature [10] is one of the most popular and reference material having SOMT and crystalline structure. Some crystalline-structured Gd-based magnetocaloric materials having giant MCE have been studied by researchers [3, 11]. However, since the price of Gd is high and its corrosion resistance is low, researchers have concentrated on both more effective and lower cost alloy systems such as amorphous and Heusler alloys.

Among amorphous alloys, Fe-based metallic glasses which have some particular properties which are important for the magnetocaloric applications (low magnetic hysteresis, high electrical resistivity, enhanced corrosion resistance, good mechanical properties) are more desirable since they can be used in a variety of industrial applications [12]. Since obtaining metallic glasses needs more than 10^5 K/s high cooling rates, literature related to Fe-based metallic glasses is limited and thin ribbons are mostly preferred by researchers. Although various soft-magnetic bulk metallic glasses (BMGs) with high GFA have recently been produced, they are not suitable for room temperature refrigeration applications because of their high T_C (450 K-550 K) [13]. As mentioned before, T_C can be tuned by adding some metals (Mn, Cr, Nb, Zr, Ce, Mo, etc) [14-21] to Fe- and Co- based alloys or compounds with/without rare earth elements so that T_C can be shifted to room temperature.

In this work, Fe-based $Fe_{68}Tb_5B_{23}Nb_4$ BMG is preferred as a base alloy since glassy rods of ~3 mm in diameter can be obtained. The measured T_C for base alloy is 487 K which is far from room temperature. In order to adjust T_C to the room temperature, Gd is partially substituted with Fe. The best GFA was obtained for x = 2, whereas for x = 6, amorphous structure could not be obtained. Some magnetocaloric properties, such as $(-\Delta S_M)^{max}$ and RC, were calculated and compared with each other and the materials studied by other researchers.

2. Experimental

The Fe-based $Fe_{68-x}Gd_xTb_5B_{23}Nb_4$ (x = 0, 2, and 6) samples were prepared by arc-melting the mixtures of 99.9 % (at.%) pure elements in Zr-gettered argon atmosphere. Ingots were remelted at least five times to get homogeneity. Then, samples were put into arc melter to reheat and suck suddenly them into a special conical shaped copper mould whose diameter changes from 1 to 3 mm (1 mm at the bottom and 3 mm at the top) to observe critical diameters. The maximum diameter of the glassy structure was obtained 3 mm for $Fe_{66}Gd_2Tb_5B_{23}Nb_4$. The structures of as-quenched samples were identified by X-ray diffraction (XRD) with CuKα radiation. The glass transition temperature (T_g) and crystallisation temperature (T_x) were measured with NETZSCH STA 449F3 differential scanning calorimetry (DSC) under flowing high purity argon gas with 15-25 mg samples at a ramp rate of 20 K/min. MicroSense EZ9 vibrating sample magnetometer (VSM) was used to measure the magnetic properties of the BMGs. The temperature dependence of magnetisation (*M*–*T*) curves from 300 K to 650 K for $Fe_{68-x}Gd_xTb_5B_{23}Nb_4$ (x = 0, 2, and 6) samples were measured under a field of 0.01 T. Moreover, the isothermal initial magnetisation curves (*M*–*H*) were measured from 300 K to 530 K for $Fe_{68-x}Gd_xTb_5B_{23}Nb_4$ (x = 0, 2 and 6) under a field of 0-2 T.

3. Results and Discussion

XRD patterns for the $Fe_{68-x}Gd_xTb_5B_{23}Nb_4$ (x = 0, 2 and 6) are shown in Fig. 1. As seen from the figure, the samples exhibit a typical broad diffraction peak between 30° and 50° of an amorphous structure with no detectable sharp Brag peak except $Fe_{62}Gd_6Tb_5B_{23}Nb_4$ for which amorphous structure could not be obtained. The XRD pattern related to $Fe_{62}Gd_6Tb_5B_{23}Nb_4$ sample reveal Bragg peaks corresponding to $(Fe,Nb)_{23}B_6$-type metastable phase and other accompanying phases (*α*-Fe, FeGdNbB, etc.) [22]. Therefore, x = 2 can be considered as the optimum Gd alloying content to achieve the amorphous structure among the $Fe_{68-x}Gd_xTb_5B_{23}Nb_4$ (x = 2 and 6) alloys. By using DSC curves, the glass transition temperature (T_g),

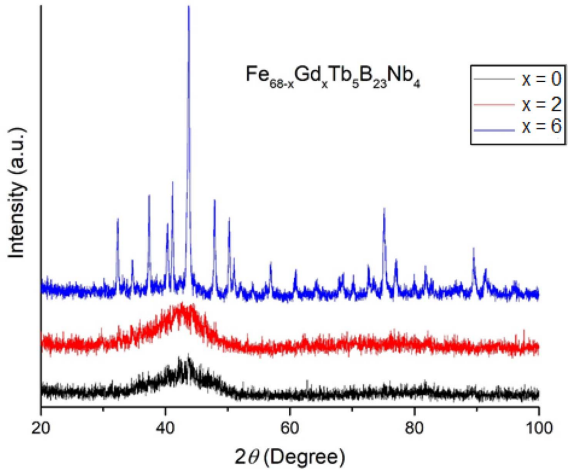

Fig. 1. (Color online) XRD patterns of $Fe_{68-x}Gd_xTb_5B_{23}Nb_4$ (x = 0, 2 and 6).

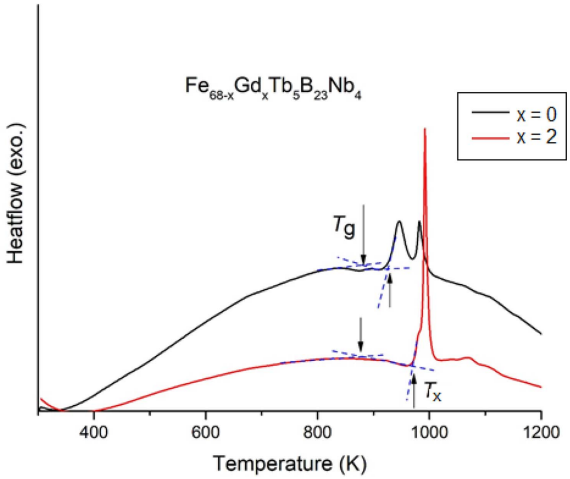

Fig. 2. (Color online) DSC heating curves for $Fe_{68-x}Gd_xTb_5B_{23}Nb_4$ (x = 0 and 2) glassy alloys.

crystallisation temperature (T_x) and supercooled liquid region were obtained for $Fe_{68-x}Gd_xTb_5B_{23}Nb_4$ (x = 0 and 2) as shown in Fig. 2. Upon heating, $Fe_{68}Tb_5B_{23}Nb_4$ and $Fe_{66}Gd_2Tb_5B_{23}Nb_4$ metallic glasses show a glass transition, followed by a clear supercooled liquid region and crystallisation. While the Gd content in $Fe_{68-x}Gd_xTb_5B_{23}Nb_4$ increases from x = 0 to 2, T_g increases from 882 to 898 K and T_x increases from 926 to 974 K, respectively. Despite the small variations in Gd content, an abrupt increase of supercooled liquid region ($\Delta T_x = T_x - T_g$) to 76 K is attained for x = 2 alloy with the high GFA, which is 32 K higher than that of the base alloy (x = 0). The $Fe_{68-x}Gd_xTb_5B_{23}Nb_4$ (x = 0, 2, and 6) samples show good soft magnetic properties near the room temperature. Magnetic hysteresis curves given in Fig. 3 for $Fe_{68-x}Gd_xTb_5B_{23}Nb_4$ (x = 0, 2, and 6) were obtained at room temperature. For $Fe_{68-x}Gd_xTb_5B_{23}Nb_4$ (x = 0, 2, and 6) saturation magnetisation (M_s) and coercivity (H_c) values are 93, 56, and 26 emu/g and 80, 100, and 120 A/m, respectively. In order to determine the magnetic transition temperatures, *M-T*

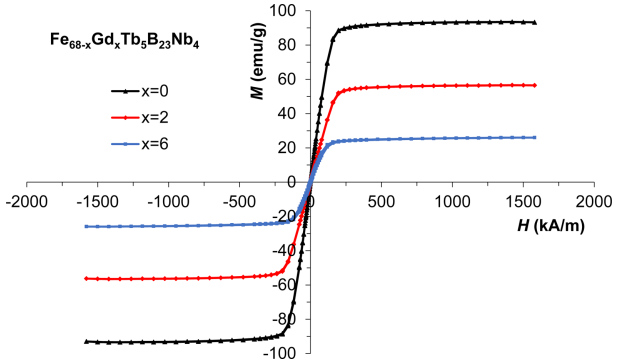

Fig. 3. (Color online) Hysteresis loops for $Fe_{68-x}Gd_xTb_5B_{23}Nb_4$ (x = 0, 2 and 6).

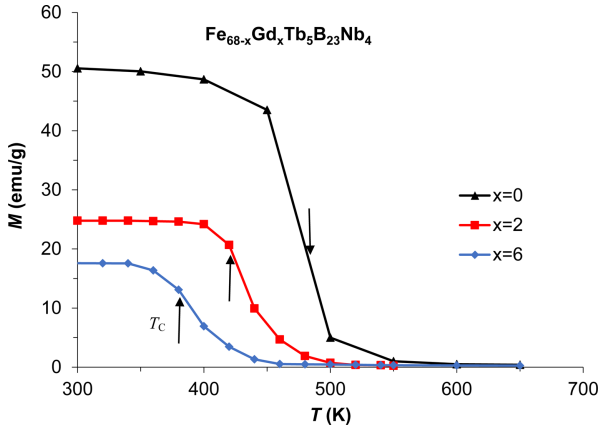

Fig. 4. (Color online) Temperature dependencies of magnetization for $Fe_{68-x}Gd_xTb_5B_{23}Nb_4$ (x = 0, 2 and 6) under a magnetic field of 0.01 T between 300 and 650 K.

measurements were performed under a field of 0.01 T and results are shown in Fig. 4. As shown in the Fig. 4, as Gd content increases the magnetic transition temperature which was determined from the minimum of the d*M*/d*T* versus *T* curve of $Fe_{68-x}Gd_xTb_5B_{23}Nb_4$ (x = 0, 2, and 6) shifts from 487 K to 420 K and 380 K, respectively. Therefore, by exchanging Gd with Fe partially, T_C could effectively be tuned in a quite broad temperature range while GFA decreased dramatically. In order to examine the magnetocaloric properties for the $Fe_{68-x}Gd_xTb_5B_{23}Nb_4$ (x = 0, 2 and 6) samples, their isothermal magnetisation curves were measured in the temperature range of 290-700 K. The samples were positioned so as to their cross-section is perpendicular to the magnetic field direction in order to take the effect of demagnetizing fields into account on the magnetic cooling [19]. Isothermal magnetisation curves measured under magnetic fields up to 2 T for $Fe_{68-x}Gd_xTb_5B_{23}Nb_4$ (x = 0, 2 and 6) are presented in Fig. 5. Since the density of domain-wall pinning sites is low in number, magnetisation saturates at low magnetic fields below the T_C [23]. However, there is a linear relationship between initial magnetisation and temperature near and above T_C. This indicates that there is a transition from ferromagnetic to paramagnetic phase. Maxwell equation was used to calculate ΔS_M from magnetisation isotherms [24]:

$$\Delta S_M = \mu_0 \int_0^{H_{max}} \left(\frac{\partial M}{\partial T} \right)_H dH \quad (1)$$

where μ_0 is the permeability of vacuum and H_{max} is the maximum applied field. The temperature dependence of $-\Delta S_M$ in $Fe_{68-x}Gd_xTb_5B_{23}Nb_4$ (x = 0, 2, 6) samples under a magnetic field change of 2 T is illustrated in Fig. 6. All samples show a broad peak centered near T_C. As the Gd

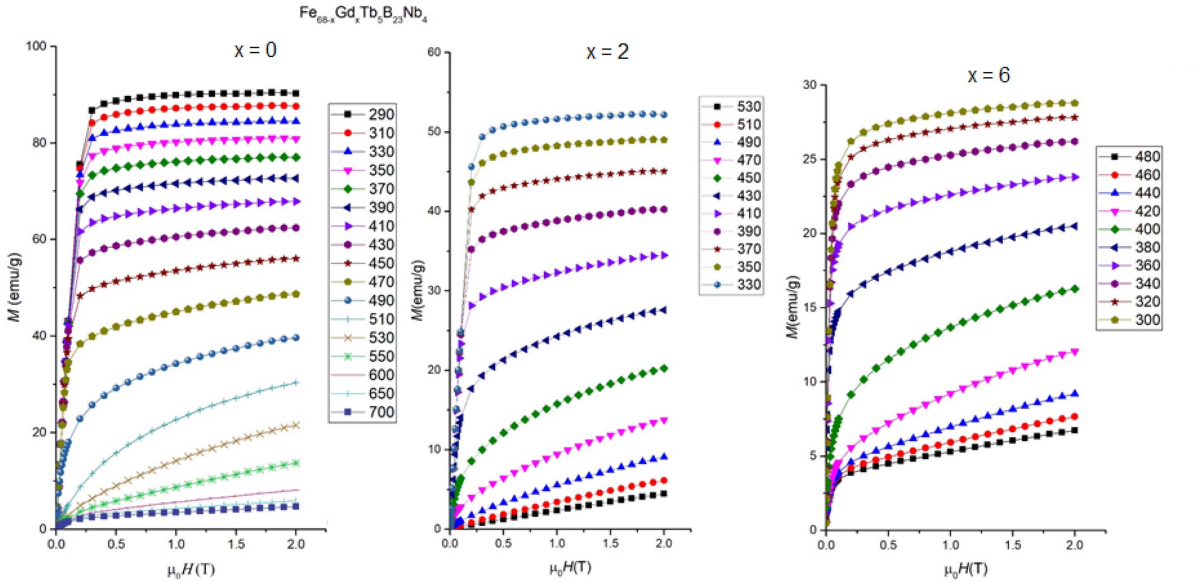

Fig. 5. (Color online) Magnetization isotherms for $Fe_{68-x}Gd_xTb_5B_{23}Nb_4$ (x = 0, 2 and 6).

content increases from 0 to 6 at.%, the temperature of maximum entropy $(T)^{max}$ for alloys with Gd changes from 480 K to 380 K and $(-\Delta S_M)^{max}$ changes from 1.16 to 0.54 $Jkg^{-1}K^{-1}$, respectively. There is a correlation between the magnetic moment of the alloys and the $-\Delta S_M$ values [25-27]. So, the reason for the decrease in $(-\Delta S_M)^{max}$ is attributed to reduce in the average magnetic moment with increasing Gd content [15]. It was found that for $Fe_{68-x}Gd_xTb_5B_{23}Nb_4$ (x = 0, 2, and 6) alloy system, while Gd content was increased, T_C shifted to the lower temperature values. However, as reported before for some Fe-Gd alloys [15, 28], T_C shifted to the higher temperatures with increase in Gd content.

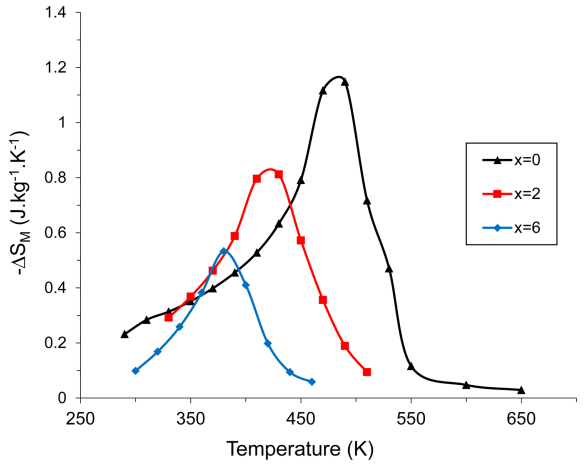

Fig. 6. (Color online) Temperature dependence of magnetic entropy change for $Fe_{68-x}Gd_xTb_5B_{23}Nb_4$ (x = 0, 2, and 6) under an applied magnetic field of 0-2 T.

Equation (2) was used to calculate refrigerant capacity [29]:

$$RC_{FWHM} = (-\Delta S_M)^{max}.\partial T_{FWHM} \quad (2)$$

where ∂T_{FWHM} is defined as the temperature interval of the full width at half maximum of the $-\Delta S_M(T)$ curve. The values of RC_{FWHM} for $Fe_{68-x}Gd_xTb_5B_{23}Nb_4$ are 116, 84.84, and 40.50 J/kg for x = 0, 2, and 6, respectively. Magnetic field dependence of $(-\Delta S_M)^{max}$ should be understood by theoretical analysis. The field variation of $(-\Delta S_M)^{max}$ can be written as a power law of the magnetic field strength [29]:

$$(-\Delta S_M)^{max} \propto H^n \quad (3)$$

To calculate the value of "n" parameter, data obtained experimentally were fitted to an exponential function. In

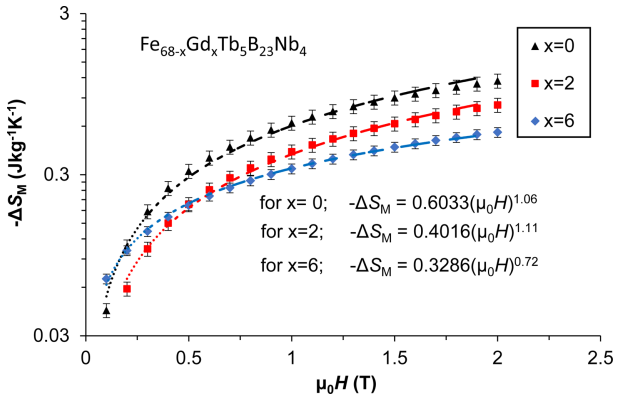

Fig. 7. (Color online) Experimental and fitted data by using Equation (3) for $Fe_{68-x}Gd_xTb_5B_{23}Nb_4$ (x = 0, 2, and 6).

Table 1. T_C, $(-\Delta S_M)^{max}$, RC values of $Fe_{68-x}Gd_xTb_5B_{23}Nb_4$ (x = 0, 2, and 6) and previously fabricated Fe-based metallic glasses for 0-2 T applied field changes.

Nominal composition	T_C (K)	$(-\Delta S_M)^{max}$ ($Jkg^{-1}K^{-1}$)	RC (J/kg)	Ref.
		0-2 T		
$Fe_{66}Gd_2Tb_5B_{23}Nb_4$	420	0.84	84.84	This work
$Fe_{62}Gd_6Tb_5B_{23}Nb_4$	380	0.54	40.5	This work
$Fe_{68}Tb_5B_{23}Nb_4$	487	1.16	116	This work
$Fe_{62}Mn_{18}P_{10}B_7C_3$	222	0.71	87.68	20
$Fe_{65}Mn_{15}P_{10}B_7C_3$	292	1.12	147.09	20
$Fe_{67}Mn_{13}P_{10}B_7C_3$	339	1.24	127.57	20
$Fe_{66}Cr_2Tb_5B_{23}Nb_4$	410	1.02	82.16	21
$Fe_{64}Cr_4Tb_5B_{23}Nb_4$	368	0.81	76.95	21
$Fe_{62}Cr_6Tb_5B_{23}Nb_4$	320	0.56	54.15	21
$Fe_{80}B_{10}Zr_9Cu_1$	356	1.72	141.4	30
$Fe_{77}Ni_3B_{10}Zr_9Cu_1$	385	1.61	119.3	30
$Fe_{75}Ni_5B_{10}Zr_9Cu_1$	408	1.58	123.5	30
$Fe_{77}Ta_3B_{10}Zr_9Cu_1$	336	1.47	123.9	30
$Fe_{75}Ta_5B_{10}Zr_9Cu_1$	313	1.04	92.2	30

this study, the $(-\Delta S_M)^{max}$ values of $Fe_{68-x}Gd_xTb_5B_{23}Nb_4$ (x = 0, 2 and 6) were fitted from 0 to 2 T by using Equation (3). It was understood that the experimental data were in a good coherence with fitting curves from 0 to 2 T as shown in Fig. 7. The exponent "n" is calculated as 1.06, 1.11 and 0.72 for $Fe_{68-x}Gd_xTb_5B_{23}Nb_4$ (x = 0, 2 and 6) respectively. While the value of exponent "n" predicted from the mean-field theory is approximately 2/3, higher values for "n" were obtained in our samples because of the distribution of T_C [3]. This may be because of local inhomogeneity existent in these alloys [31].

Table 1 shows the T_C, $(-\Delta S_M)^{max}$ and RC values obtained from our samples and some previously fabricated Fe-based metallic glass magnetocaloric materials under the applied field of 0-2 T. Although T_C could be tuned near to the room temperature for our alloys, RC values decreased. However, these values are still comparable with those of previously casted Fe-based metallic glasses. This reduction may result from the decrease in the percentage composition of ferromagnetic atoms in the alloys.

4. Conclusion

Magnetocaloric and soft magnetic properties of $Fe_{68-x}Gd_xTb_5B_{23}Nb_4$ (x = 0, 2, 6) metallic glasses were investigated. Maximum GFA was obtained for $Fe_{66}Gd_2Tb_5B_{23}Nb_4$. However, GFA was decreased by exchanging 6 % Gd with Fe. Under the applied magnetic field change of 2 T, the $(-\Delta S_M)^{max}$ and RC values decrease when the Gd content is increased in the alloy system. As Gd is replaced by Fe partially, T_C decreases from 480 K (for x = 0) to 420 K (for x = 2) and 380 K (for x = 6) respectively. Magnetocaloric properties for our samples are comparable with those of previously developed BMGs given in Table 1. These findings show that the successful synthesis of the Fe-based $Fe_{68-x}Gd_xTb_5B_{23}Nb_4$ (x = 0, 2, and 6) could be considered as promising candidates as magnetic refrigerant materials since samples have good MCE response, negligible hysteresis, tunable T_C and good thermal stability.

References

[1] P. Weiss and Le phénoméne magnétocalorique, Piccard A. J. Phys. Theor. Appl. **7**, 103 (1917).

[2] P. Weiss and Sur un nouveau phénoméne magnétocalorique, Piccard A. Comptes Rendus. **166**, 352 (1918).

[3] V. K. Pecharsky and Jr. K. A. Gschneidner, Phys. Rev. Lett. **78**, 4494 (1997).

[4] F. X. Hu, B. G. Shen, J. R. Sun, Z. H. Cheng, G. H. Rao, and X. X. Zhang, Appl. Phys. Lett. **78**, 3675 (2001).

[5] F. Guillou, G. Porcari, H. Yibole, N. Van Dijk, and E. Brück, Adv. Mater. **26**, 2671 (2014).

[6] 29th Informatory Note on Refrigeration Technologies/ November 2015 The Role of Refrigeration in the Global Economy.

[7] P. Yu, N. Z. Zhang, Y. T. Cui, L. Wen, Z. Y. Zeng, and L. Xia, J. Alloys Compd. **655**, 353 (2016).

[8] A. Kitanovski, U. Plaznik, U. Tomc, and A. Poredoš, Int. J. Refrig. **57**, 288 (2015).

[9] A. M. Tishin, E. V. Zatsepina, P. W. Egolf, and D. Vuarnoz, (2009) In: Proceedings of third IIF-IIR international conference on magnetic refrigeration at room temperature, Des Moines, 11-15 May.

[10] S. Y. Dan'kov, A. Tishin, V. Pecharsky, and K. Gschneidner, Phys. Rev. B - Condens Matter Mater Phys. **57**, 3478 (1998).

[11] V. Provenzano, A. J. Shapiro, and R. D. Shull, Nature **429**, 853 (2004).

[12] I. Kucuk, K. Sarlar, A. Adam, and E. Civan, Philos. Mag. **96**, 3120 (2016).

[13] J. Li, J. Y. Law, H. Ma, A. He, Q. Man, H. Men, J. Huo, C. Chang, X. Wang, and R. W. Li, J. Non. Cryst. Solids **425**, 114 (2015).

[14] Y. K. Fang, C. C. Yeh, C. C. Hsieh, C. W. Chang, H. W. Chang, W. C. Chang, X. M. Li, and W. J. Li, Appl. Phys. **105**, 07A910 (2009).

[15] J. Y. Law, R. V. Ramanujan, and V. Franco, J. Alloys Compd. **508**, 14 (2010).

[16] R. Yapp, B. E. Watts, and F. Leccabue, J. Magn. Magn. Mater. **215**, 300 (2000).

[17] P. Álvarez-Alonso, J. D. Santos, M. J. Pérez, C. F. Sánchez-Valdes, J. L. Sánchez Llamazares, and P. Gorria, J. Magn. Magn. Mater. **347**, 75 (2013).

[18] H. C. Tian, X. C. Zhong, Z. W. Liu, Z. G. Zheng, and J. X. Min, Mater. **138**, 64 (2015).
[19] M. Zhang, J. Li, F. Kong, and J. Liu, Intermetallics **59**, 18 (2015).
[20] H. Zhang, R. Li, T. Xu, F. Liu, and T. Zhang, J. Magn. Magn. Mater. **347**, 131 (2013).
[21] E. Civan, K. Sarlar, and I. Kucuk, Philos Mag. **97**, 1464 (2017).
[22] A. Hirata, Y. Hirotsu, K. Amiya, N. Nishiyama, and A. Inoue, Mater. Sci. Forum. 539-543, 2077-2081 (2007).
[23] T. Bitoh, A. Makino, and A. Inoue, J. Appl. Phys. **99**, 08F102 (2006).
[24] T. Hashimoto, T. Numasawa, M. Shino, and T. Okada, Cryogenics (Guildf). **21**, 647 (1981).
[25] V. Franco, C. F. Conde, J. S. Blázquez, A. Conde, P. Švec, D. Janičkovič, and L. Kiss, J. Appl. Phys. **101**, 093903 (2007).
[26] Y. Wang and X. Bi, Appl. Phys. Lett. **95**, 262501 (2009).
[27] R. Caballero-Flores, V. Franco, A. Conde, and L. F. Kiss, J. Appl. Phys. **105**, 07A919 (2009).
[28] K. Yano, Y. Akiyama, K. Tokumitsu, E. Kita, and H. Ino, J. Magn. Magn. Mater. **214**, 217 (2000).
[29] V. Franco, J. S. Blázquez, and A. Conde, Appl. Phys. Lett. **89**, 222512 (2006).
[30] X. C. Zhong, H. C. Tian, S. S. Wang, Z. W. Liu, Z. G. Zheng, and D. C. Zeng, J. Alloys Compd. **633**, 188 (2015).
[31] W. H. Wang, M. X. Pan, D. Q. Zhao, Y. Hu, and H. Y. Bai, J. Phys. Condens. Matter. **16**, 3719 (2004).